



theoretical underpinnings of phantom phenomenology are still under investigations as many of such theories may suffer from instabilities. The viable Bimetric gravity can also show phantom behaviour in some of their parameter space. Providing an effective  $\Lambda$ -like effect and the possibility of phantom behaviour can make Bimetric gravity suitable for investigation as a possible solution for the Hubble tension.

In the literature, there are not many studies related to the effect of Bimetric gravity on the large-scale structure formation in the universe. In particular, the effects of modification of gravity at cosmological scales in higher-order clustering are still mostly unknown. One of the important parameters related to higher order clustering is the ‘‘skewness’’ parameter [29]. This is defined as the ‘‘normalized third order moment in count-in-cells statistics’’ which can describe the non-Gaussian feature in the probability distribution of the perturbed matter field. In a purely matter-dominated Einstein-de Sitter Universe, one gets  $S_3 \approx 34/7 \approx 4.857$ . Any observed deviation from this value can be a signature for a modified gravity model [30].

Our aim in this work is to study the linear and second-order perturbations for a specific class of Bimetric gravity models and illustrate the effects of these modifications to gravity on observables related to perturbed Universe such as  $f\sigma_8$ , skewness parameter  $S_3$  and Integrated Sachs-Wolfe (ISW) effect and compare the results with concordance  $\Lambda$ CDM models. This can be particularly interesting in the context of results from future surveys like Euclid which can provide an accurate measurement of the skewness parameter and can potentially distinguish  $\Lambda$ CDM model from different modified gravity models including the Bimetric gravity.

This paper is organized as follows: in section II, we briefly describe the theory of Bimetric gravity; in section III, we describe the perturbation theory formalism used for the Bimetric gravity and the discuss the effects of these perturbations on observables in respective subsections III B. Data constraints are obtained in section IV. In section V, we study ISW effect through galaxy-temperature cross-correlations. We conclude with a discussion in the last section.

## II. BIMETRIC GRAVITY & COSMOLOGY

Bimetric gravity is the theory of two interacting spin-2 fields, one massive and one massless. An interacting symmetric spin-2 field  $f_{\mu\nu}$  is introduced together with the physical metric  $g_{\mu\nu}$ , which is a massless spin-2 field. The standard matter particles and fields are coupled to the physical metric  $g_{\mu\nu}$  only. For ghost-free Bimetric gravity, where both metrics are dynamical, action can be written as [17, 19]

$$S = - \int d^4x \sqrt{-g} \frac{R}{2m_g} - \int d^4x \sqrt{-f} \frac{\tilde{R}}{2m_f} + m^4 V(g_{\mu\nu}, f_{\mu\nu}) + \int d^4x \sqrt{-g} L_m, \quad (1)$$

where  $R$  and  $\tilde{R}$  are Ricci scalars for  $g_{\mu\nu}$  and  $f_{\mu\nu}$ .  $m_g$  and  $m_f$  are the Planck’s mass for the metrics  $g_{\mu\nu}$  and  $f_{\mu\nu}$  respectively.  $V$  is the interaction term which has the parametric form as

$$V = \sum_{n=0}^4 \beta_n e_n(\chi), \quad (2)$$

where

$$\chi = \sqrt{g^{-1}f}. \quad (3)$$

Here  $e_n(\chi)$  is the elementary symmetry polynomials of eigenvalues of the matrix  $\chi$  which can be written as follows

$$\begin{aligned} e_0(\chi) &= 1, & e_1(\chi) &= [\chi], & e_2(\chi) &= \frac{1}{2}([\chi]^2 - [\chi^2]) \\ e_3(\chi) &= \frac{1}{6}([\chi]^3 - 3[\chi][\chi^2] + 2[\chi^3]), & e_4(\chi) &= \det(\chi) \end{aligned} \quad (4)$$

where,  $[\chi]$  is the trace of the matrix  $\chi$  and  $\det(\chi)$  is the determinant of  $\chi$ . The Bimetric gravity is characterized by 5 constants  $\beta_i$ . Under the scaling transformation  $f_{\mu\nu} \rightarrow \frac{m_g^2}{m_f^2} f_{\mu\nu}$  and  $\beta_n \rightarrow \left(\frac{m_f}{m_g}\right)^n \beta_n$ , we can make  $M_*^2 = 1$  where,  $M_* = m_f/m_g$ . Hence  $M_*$  is not a free parameter. In what follows, we consider  $M_*^2 = 1$  and  $m_g = m_f$ . With such rescaling [31], it is common to work in terms of dimensionless quantities which remain same under these scaling. Here we use the definitions and parameterisation of Dhawan et. al [19] to write the dimensionless parameters as

$$B_i \equiv \frac{m^2 \beta_i}{H_0}. \quad (5)$$

There are various possible models depending on which  $B$ s are non-zero. For simplicity, here we consider models with only  $B_0$  and  $B_1$  nonzero. Cosmological expansion for these models is given by [32]

$$\frac{H^2}{H_0^2} = \frac{\Omega_m(1+z)^3}{2} + \frac{B_0}{6} + \sqrt{\left(\frac{\Omega_m(1+z)^3}{2} + \frac{B_0}{6}\right)^2 + \frac{B_1^2}{3}}, \quad (6)$$

where due to spatial flatness condition, the parameter  $B_0$  can be written in terms of other two parameters  $\Omega_m$  and  $B_1$  as

$$B_0 = 3 \left(1 - \Omega_m - \frac{B_1^2}{3}\right), \quad (7)$$

where  $\Omega_m$  is the present day matter density parameter. As one can see in equation 6, the model naturally gives a cosmological constant term  $\frac{B_0}{3}$  in the Universe which can be positive or negative depending on the values of  $\Omega_m$  and  $B_1$ . This originates from the interacting potential itself. For early times  $z \rightarrow \infty$ ,

$$\frac{H^2}{H_0^2} \approx \Omega_m(1+z)^3 + \frac{B_0}{3}, \quad (8)$$

which is  $\Lambda$ CDM model. For future infinity ( $z \rightarrow -1$ ),

$$\frac{H^2}{H_0^2} \approx \text{constant}, \quad (9)$$

and hence a de-Sitter or anti-de-Sitter model.

Using the above equations and comparing them with the standard model, we can derive an expression for the effective dark energy equation of state ( $w_{de}$ ). We plot  $w_{de}(z)$  as a function of redshift( $z$ ) in figure 1 and observe that the Bimetric gravity can show phantom behavior. In the figure 2, where we show the dependence of  $w_{de}(z=0)$  on  $B_1$  and  $\Omega_{m0}$ , it is evident that Bimetric gravity shows phantom behavior at present for a large range of parameter values and can provide a possible theoretical basis for parametric phantom models, which people have recently considered [27, 33] to alleviate the cosmological tensions.

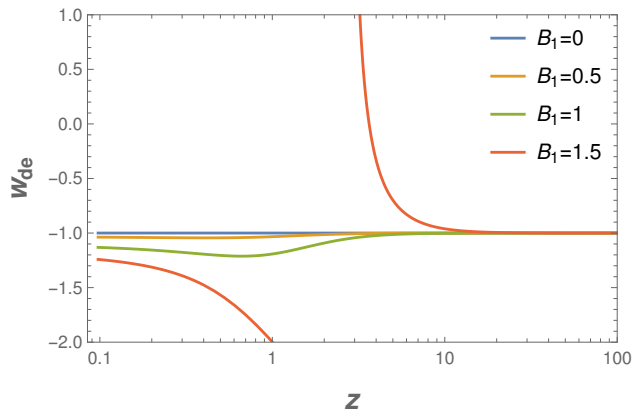


FIG. 1: Equation of state  $w_{de}$  for different values of parameter  $B_1$ .

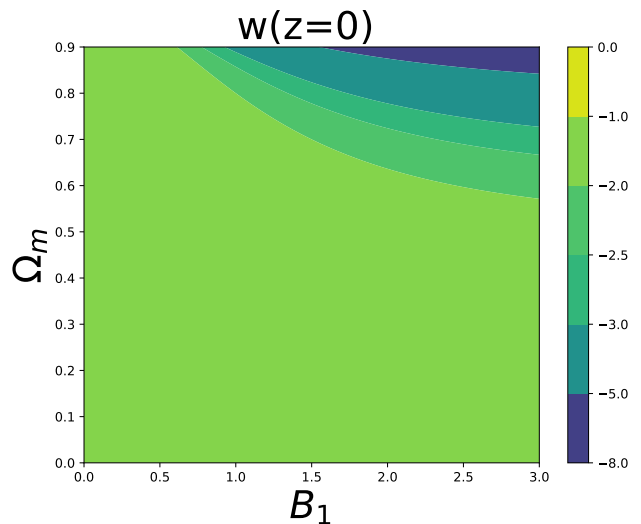


FIG. 2: Present day  $w$  as a function of  $B_1$  and  $\Omega_{m0}$ .

### III. GROWTH OF PERTURBATIONS AND LARGE SCALE STRUCTURE

Next we study the effects of Bimetric gravity on the growth of matter perturbations. We study linear perturbations as well as second-order perturbations. Second-order perturbations affect the skewness ( $S_3$ ) of the matter density field. We study the effects of modified theory parameters on skewness. We use the formalism of Multamaki et al. [34] to study the growth of matter perturbations but one can also use the formalism for modified gravity models by Lue et al. [35] and both of them give similar results.

### A. Formalism & Equations

We start with the formalism of Multamaki et al. [34], wherein Raychaudhuri's equation is used to derive a general equation for the growth of perturbations at large scales. We should point out that Bimetric gravity is a modified theory of gravity containing only pressure-less matter in the energy budget of the Universe at late times (one can ignore the contribution from radiation at late times). The formalism developed by Multamaki et al. [34] to study the matter density perturbations for such modified theory of gravity is briefly discussed below.

The Raychaudhuri's equation for a shearless and irrotational field  $v^\mu$  is given by

$$\dot{\Theta} + \frac{\Theta^2}{3} = R_{\mu\nu}v^\mu v^\nu, \quad (10)$$

where

$$\Theta = \nabla_\mu v^\mu, \quad \theta = \nabla_i v^i. \quad (11)$$

As shown in [34], this can be related to average Hubble expansion rate ( $\bar{H}$ ) and locally perturbed expansion rate  $H$  as

$$\frac{\dot{\theta}}{a} + \frac{\theta}{a}\bar{H} + \frac{\theta^2}{3a^2} = 3(\dot{H} + H^2 - \dot{\bar{H}} - \bar{H}^2). \quad (12)$$

Combining the above equation with the continuity equation for pressure-less matter

$$\frac{\partial\delta}{\partial t} + (1 + \delta)\theta = 0, \quad (13)$$

where  $\delta$  is the matter overdensity. We get the evolution equation for  $\delta$  [34] as

$$\frac{d^2\delta}{d\eta^2} + \left(2 + \frac{\dot{\bar{H}}}{\bar{H}^2}\right) \frac{d\delta}{d\eta} - \frac{4}{3} \frac{1}{1 + \delta} \left(\frac{d\delta}{d\eta}\right)^2 = -3 \frac{1 + \delta}{\bar{H}^2} \left[ (\dot{H} + H^2) - (\dot{\bar{H}} + \bar{H}^2) \right], \quad (14)$$

where overdot represents derivative w.r.t. time and  $\eta \equiv \ln(a)$ . Quantities with overbar represent background quantities. Following [34], we can expand the r.h.s of equation (14) as

$$3 \frac{1 + \delta}{\bar{H}^2} \left[ (\dot{H} + H^2) - (\dot{\bar{H}} + \bar{H}^2) \right] = 3(1 + \delta) \sum_{n=1} c_n \delta^n. \quad (15)$$

We further expand  $\delta$  as [34]

$$\delta = \sum_{i=1}^{\infty} \frac{D_i(\eta)}{i!} \delta_0^i, \quad (16)$$

where  $\delta_0$  is the small perturbation. With this we get the linear and second-order perturbation equations as [34]

$$D_1'' + \left(2 + \frac{\dot{\bar{H}}}{\bar{H}^2}\right) D_1' + 3c_1 D_1 = 0, \quad (17)$$

and

$$D_2'' + \left(2 + \frac{\dot{\bar{H}}}{\bar{H}^2}\right) D_2' - \frac{8}{3} D_1'^2 + 3c_1 D_2 + 6(c_1 + c_2) D_1^2 = 0. \quad (18)$$

For Bimetric gravity, which we are considering here, we get

$$c_1 = \frac{-\frac{2\Omega_m}{a^3} \left(\frac{\Omega_m}{2a^3} + \frac{B_0}{6}\right) \left(\left(\frac{\Omega_m}{2a^3} + \frac{B_0}{6}\right)^2 + \frac{B_1^2}{3}\right) - \frac{2\Omega_m}{a^3} \left(\left(\frac{\Omega_m}{2a^3} + \frac{B_0}{6}\right)^2 + \frac{B_1^2}{3}\right)^{3/2} - \frac{\Omega_m^2 B_1^2}{a^6}}{8 \left(\frac{\Omega_m}{2a^3} + \frac{B_0}{6} + \sqrt{\left(\frac{\Omega_m}{2a^3} + \frac{B_0}{6}\right)^2 + \frac{B_1^2}{3}}\right) \left(\left(\frac{\Omega_m}{2a^3} + \frac{B_0}{6}\right)^2 + \frac{B_1^2}{3}\right)^{3/2}}, \quad (19)$$

and

$$c_2 = \frac{-8\Omega_m^2 B_1^2 \left( \left( \frac{\Omega_m}{2a^3} + \frac{B_0}{6} \right)^2 + \frac{B_1^2}{3} \right) + 9\Omega_m^3 B_1^2 \left( \frac{\Omega_m}{2a^3} + \frac{B_0}{6} \right)}{96 \left( \frac{\Omega_m}{2a^3} + \frac{B_0}{6} + \sqrt{\left( \frac{\Omega_m}{2a^3} + \frac{B_0}{6} \right)^2 + \frac{B_1^2}{3}} \right) \left( \left( \frac{\Omega_m}{2a^3} + \frac{B_0}{6} \right)^2 + \frac{B_1^2}{3} \right)^{5/2}}, \quad (20)$$

We solve for linear and second-order perturbations for values of  $B_1$  and  $\Omega_m$ . We set the initial conditions at redshift  $z = 1000$ , assuming that model reproduces the Einstein-de Sitter Universe at that epoch. Solving these equations, the linear growth rate is shown in figure 3 while the evolution of the second-order perturbations are shown in figure 4. As shown in figure 3, for smaller values of  $B_1$ , the linear growth is similar to  $\Lambda$ CDM model. But for higher values, in particular for values  $B_1 \geq 1.4$ , there is an increase in growth around  $z \sim 1$ . This can be possibly due to some extra attractive gravitational pull provided by the Bimetric gravity for such values of  $B_1$ .

For the second order perturbation as shown in figure 4, we get the similar behaviour where the deviation from  $\Lambda$ CDM increases for larger values of  $B_1$ .

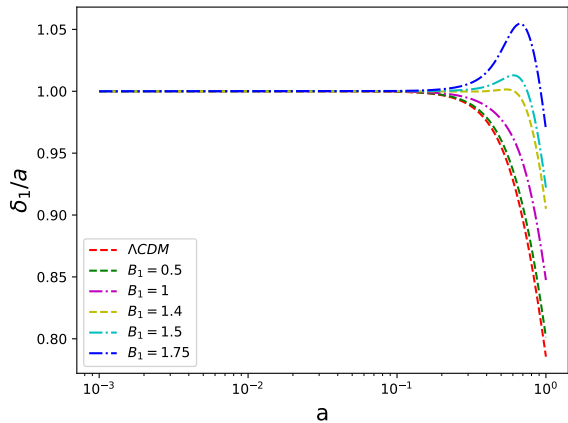


**FIG. 3:** Linear perturbations for different values of parameter  $B_1$ . For higher values of  $B_1 (> 1.4)$ , there is a very distinct feature of a brief epoch with growth faster than  $\Lambda$ CDM as well as Einstein-diSitter.

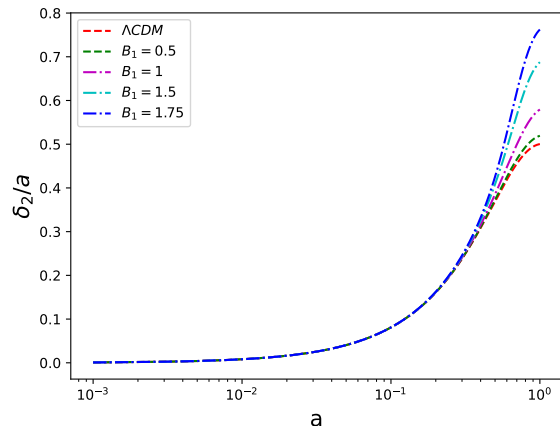


**FIG. 4:** Second order perturbations for different values of parameter  $B_1$ .

## B. Observables

### 1. $f\sigma_8$

Linear theory calculations can be used to predict the growth and clustering of structures at appropriate length scales and times. Redshift surveys provide an estimate of a combination of linear growth  $\delta$ , its derivative given by growth factor  $f$  and its rms fluctuation at the length scale of  $8h^{-1} Mpc$  given by the parameter  $\sigma_8$ . The combination  $f\sigma_8$  [36] is an important observable for perturbed Universe at linear scale. Here the growth factor  $f$  and the  $\sigma_8$  parameters are given as

$$f(a) = \frac{d(\log(\delta))}{d(\log(a))}, \quad (21)$$

and

$$\sigma_8(a) = \sigma_8(a=1) \frac{\delta(a)}{\delta(1)}. \quad (22)$$

In figure 5, we show the  $f\sigma_8$  for Bimetric gravity for the different values of the parameter  $B_1$  along with the  $\Lambda$ CDM model. We observe that we always get larger  $f\sigma_8$  for larger values of  $B_1$  compared to  $\Lambda$ CDM ( $B_1 = 0$ ). Moreover for larger values of  $B_1$ , the  $f\sigma_8$  behaviour for Bimetric gravity models are not consistent in the redshift range  $z \sim 0.25-0.5$ . In this plot, we fix the value of  $\sigma_8$  at  $z = 0$  by Planck-2018 observations [9] assuming a  $\Lambda$ CDM model. Hence for this

figure, one expects that for higher values of  $B_1$ , a lower value for  $\sigma_8$  may be necessary to make the  $f\sigma_8$  for Bimetric theory more consistent with the observational data.

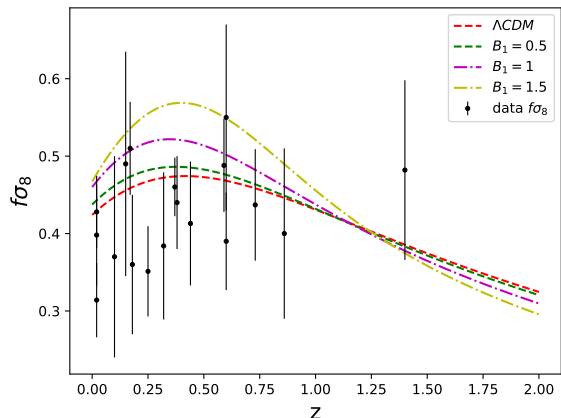


**FIG. 5:** Combination  $f\sigma_8$  as a function of redshift  $z$  for different theories. We also plot the data points from observations [37].

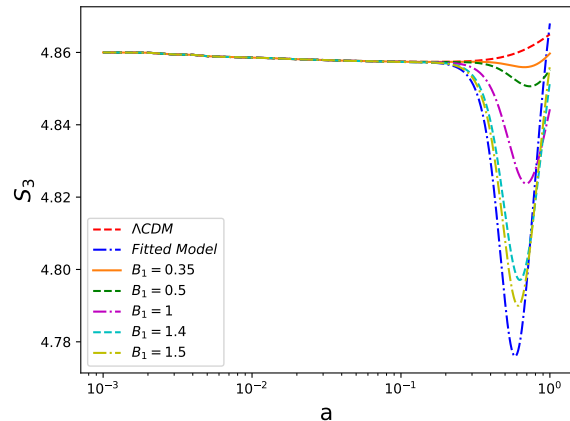


**FIG. 6:** Skewness  $S_3$  as a function of scale factor for different values of  $B_1$ .

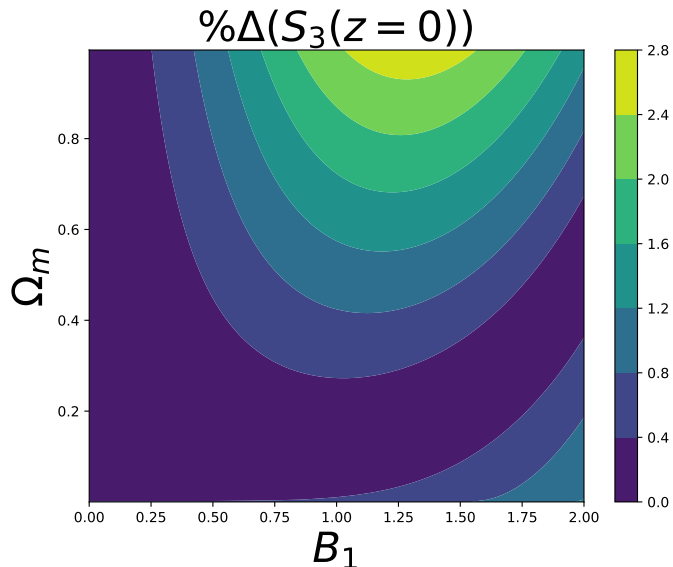


**FIG. 7:** Deviation of  $S_3$  from  $\Lambda$ CDM model for different values of  $B_1$ . While the linear growth rate and second-order perturbations show huge differences, the percentage difference in the combination probed by  $S_3$  is a few percent.

## 2. Skewness ( $S_3$ )

Second-order perturbations provide further connection with statistics of observed perturbations. Gaussian initial conditions evolve into non-gaussian distribution with time and the extent of non-gaussianity depends on dynamics of the individual fluid components of the universe or the theory of gravity which evolves the whole system. Mode coupling leads to an imbalance in the distribution of voids and overdense regions [38]. Second-order perturbations play a role in this and can be related to the skewness of the density field as [34, 38]

$$S_3 = \frac{\langle \delta^3 \rangle}{\langle \delta^2 \rangle^2}, \quad (23)$$

which can be written as

$$S_3 = 3 \frac{D_2}{D_1^2}. \quad (24)$$

$S_3$  can be sensitive to underlying dark energy characteristics [30] or modification of GR. Here we show that the growth of perturbations is sensitive to parameter  $B_1$  as we illustrate in figures 3 and 4. In figure 6, we show the evolution of  $S_3$  for different values of  $B_1$ . In figure 7 we show the present day percentage difference of  $S_3$  from  $\Lambda$ CDM model as a function of  $B_1$  and  $\Omega_{m0}$ . This can be used to distinguish the Bimetric models from the  $\Lambda$ CDM using the  $S_3$  measurements in near future.

#### IV. OBSERVATIONAL CONSTRAINTS ON BIMETRIC MODEL

Given the behaviour of Bimetric gravity in terms of different observables, we now study the observational constraints on Bimetric gravity using low redshift cosmological observations. In this regard, we do the Markov Chain Monte Carlo (MCMC) analysis using different latest cosmological observational data to put constraints on the model parameters for the Bimetric gravity. The analysis is performed using the EMCEE hammer [39], a PYTHON implementation of the MCMC sampler.

We use the following data:

- Pantheon+ and SH0ES data [40] ;
- The Gold-2017 set for the  $f\sigma_8$  data [37, 41];
- The Baryon acoustic oscillations (BAO) measurements by the completed Sloan Digital Sky Survey (SDSS) lineage of experiments on large scales [42];
- The angular diameter distances measured using water megamasers under the Megamaser Cosmology Project [43].

Parameter	Prior
$\Omega_m$	[0.0, 0.9]
$h$	[0.6, 0.8]
$B_1$	[0, 5]
$r_d$	[130, 160]
$\sigma_8$	[0.01, 0.9]
$M$	[-19.40, -19.00]

**TABLE I:** The range of the uniform priors for the parameters used for the MCMC analysis.

We use the uniform priors given in Table I for the model parameters for the Bimetric gravity. The posterior probability distributions and their corresponding confidence contours for different parameters are shown in figure (8). As one can see from this figure, a substantial deviation from  $\Lambda$ CDM model in terms of the parameter  $B_1$  is allowed by the data although the  $\Lambda$ CDM behaviour ( $B_1 = 0$ ) is still allowed. The reconstructed effective dark energy equation of state and the reconstructed  $S_3$  parameters as a function of redshifts are shown in figures (9) and (10). The constrained Bimetric model gives a phantom-like effective dark energy equation of state. The data also allows substantial deviation in the parameter  $S_3$  from  $\Lambda$ CDM model behaviour although the  $\Lambda$ CDM behaviour for  $S_3$  is also allowed in the constrained behaviour of  $S_3$ .

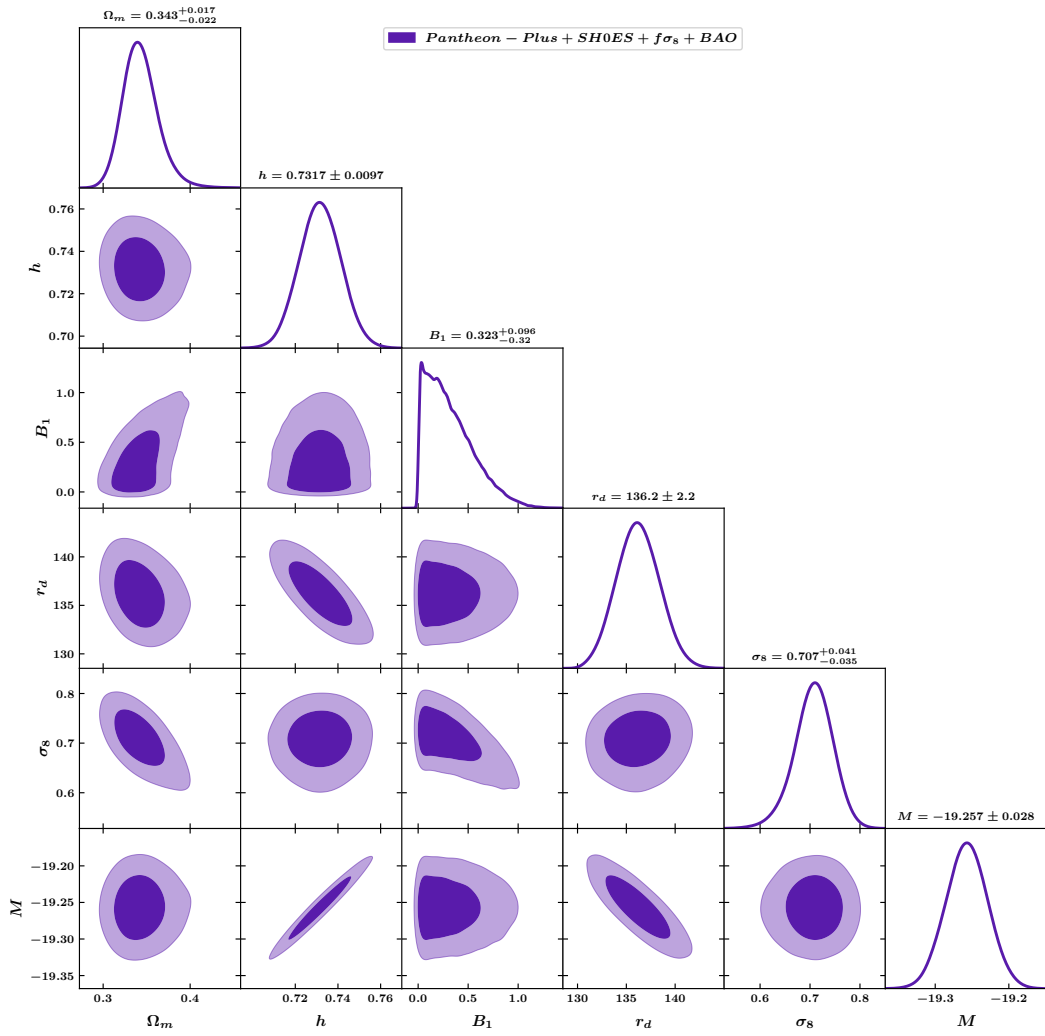


**FIG. 8:** Marginalized posterior distribution of the set of parameters  $\Omega_m$ ,  $h$ ,  $B_1$ ,  $r_d$ ,  $\sigma_8$  and  $M$  and their corresponding 2D confidence contours, obtained from the MCMC analysis for the Bimetric gravity utilizing all the data sets mentioned in section IV

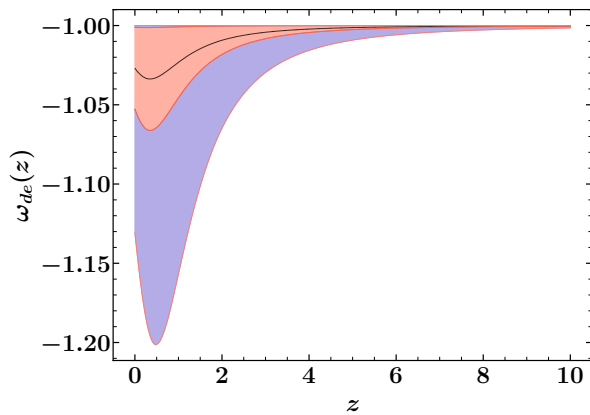


**FIG. 9:** Reconstructed equation of state  $\omega_{de}$  as a function of redshift  $z$ . Black line is the best fit value with shaded regions as  $1\sigma$  and  $2\sigma$  for the inner and the outer shaded region respectively.

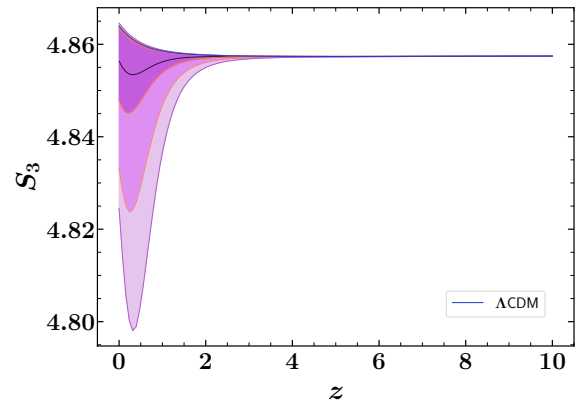


**FIG. 10:** Reconstructed skewness  $S_3$  as a function of redshift  $z$ . Black line is the best fit value with shaded regions as  $1\sigma$ ,  $2\sigma$  and  $3\sigma$  for the innermost to the outermost shaded region. Blue line is for the  $\Lambda$ CDM model.



## V. INTEGRATED SACHS WOLFE (ISW) EFFECT

Given the observational constraints on the Bimetric gravity considered in this analysis, we study how far the ISW signal in this model deviates from the  $\Lambda$ CDM model within that constraints. CMB photons traveling through evolving spacetime, traverse potentials created by matter inhomogeneity and undergo changes in their wavelengths. This contributes to anisotropies of CMB spectrum and is dubbed ISW effect [44, 45]. The effect can be detected by cross-correlation of Large Scale Structure (LSS) tracers with CMB anisotropies [35, 45–47] which can be used as a probe for theories giving dark energy effects. Here we follow the formalism of Lue et al. [35] who gave a general prescription for studying the ISW effect in modified gravity theories. We calculate the evolution of time derivatives of potentials for our Bimetric model and compare it with the standard  $\Lambda$ CDM model.

Following the prescription by Lue et al. [35], we characterize background expansion in Bimetric gravity theory by a function  $g(x)$  as

$$g(x) = \left( \frac{H}{H_0} \right)^2, \quad (25)$$

with  $x$  defined as

$$x \equiv \frac{8\pi G\rho_m}{3H_0^2}. \quad (26)$$

For example, in  $\Lambda$ CDM, the function takes the form

$$g(x) = x + \Omega_\Lambda. \quad (27)$$

For the Bimetric gravity,  $g(x)$  is given by

$$g(x) = \frac{1}{2}x + \frac{B_0}{6} + \sqrt{\left(\frac{1}{2}x + \frac{B_0}{6}\right)^2 + \frac{B_1^2}{3}}. \quad (28)$$

We start with the following convention for the perturbed metric [35]

$$ds^2 = -(1 + 2\Psi)dt^2 + a^2(1 + 2\Phi)(dr^2 + r^2d\Omega^2). \quad (29)$$

The ISW effect is proportional to a combination of temporal derivatives of potentials as

$$A(\dot{\Psi} - \dot{\Phi}) = \left[ (1 - f^{MG})(g' + (3/2)g''x) + \frac{3}{2}(5xg'' + 3x^2g''') \right] D_+, \quad (30)$$

wherein  $D_+$  is linear first order perturbation and  $f$  is growth rate defined as  $\frac{d(\ln D_+)}{d(\ln a)}$ . In figure 11, we compare this term for our constrained Bimetric gravity (for best fitted parameter values) with  $\Lambda$ CDM model as constrained by Planck-2018. We see that the observationally constrained Bimetric model does not differ much from the  $\Lambda$ CDM model.

Finally, the cross-correlated ISW signal ( $w_{gT}$ ) between LSS and CMB can be calculated as

$$w_{gT} = 3T_0\Omega_{m0}b(2\pi)^2\frac{H_0}{c^3} \int dz \sqrt{g} \quad D_+^2 \left[ (1 - f)(g' + (3/2)g''x) + \frac{3}{2}(5xg'' + 3x^2g''') \right] w_g(z) \int \frac{dk}{k} P(k) J_0(k\theta\chi). \quad (31)$$

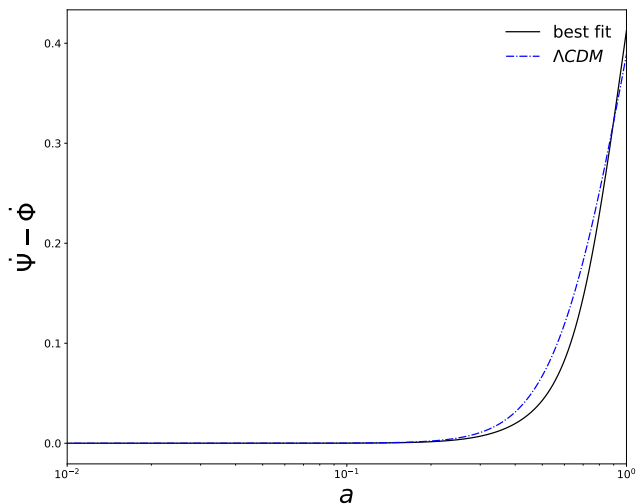


**FIG. 11:** Comparison of the evolution of temporal derivatives of the potentials. Differences in linear growth rate are translated here as well.

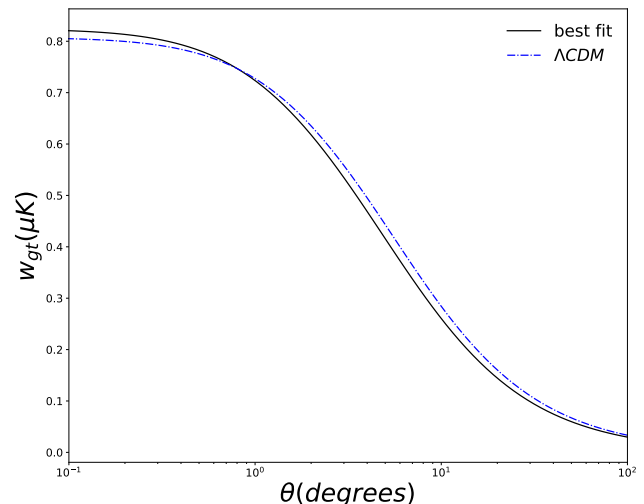


**FIG. 12:** Galaxy Temperature correlation for the best fit Bimetric model along with  $\Lambda$ CDM. The two are very similar.

Here  $T_0$  is the present CMB temperature,  $b$  is the bias factor (assumed constant here),  $P(k)$  is present-day matter power spectrum,  $\chi$  is comoving distance as a function of  $z$ ,  $J_0$  is zeroth Bessel function and  $w_g(z)$  is the survey-dependent galaxy selection function. For  $T_0$ , we take the value  $2.725\mu K$ ,  $b$  is taken from Lue et al. [35] that is 5.47. We use the  $w_g(z)$  of Takada & Jain [48] with mean redshift of 0.49.

This correlation function for best fitted Bimetric gravity as well as for  $\Lambda$ CDM model are plotted in figure 12 and it is evident that the cross-correlated ISW signal in Bimetric gravity is similar to  $\Lambda$ CDM model.

## VI. CONCLUSIONS

We study the cosmological evolution in a subclass of Bimetric gravity model, where only the parameters  $B_0$  and  $B_1$  are nonzero. We show that the effective dark energy behaviour in such a modified gravity theory can be phantom-like for a large range of parameter values. Moreover the model admits a cosmological constant that can be positive or negative depending on the values of the parameter  $B_1$  and  $\Omega_m$ . This can naturally mimic a cosmological evolution where the Universe contains a phantom like dark energy plus a negative Cosmological Constant apart from the standard matter. As shown recently such set up can be useful to solve the Hubble Tension [33].

We also study the linear and second order growth of matter fluctuations in the Bimetric gravity. We find that the growth of both linear and second order perturbations are strongly dependent on the values of parameter  $B_1$  that signifies the deviation from the corresponding  $\Lambda$ CDM limit. This results in significant deviations of observables like " $f\sigma_8$ " and "Skewness" parameter  $S_3$  from the  $\Lambda$ CDM behaviour for higher values of the parameter  $B_1$ .

With these observations, we subsequently constrain the Bimetric model with low-redshift observational data from SNIa Observation ( Pantheon+ and SH0ES), BAO observations as well as Growth measurements. It shows that the data allow significant deviation from  $\Lambda$ CDM behavior although  $\Lambda$ CDM limit of Bimetric theory ( $B_1 = 0$ ) is also consistent with the data.

Finally we calculate the ISW signal by cross-correlating the CMB and LSS signals for our best fit Bimetric gravity model and show that it is mostly similar to the  $\Lambda$ CDM model as constrained by Planck-2018.

To conclude, we show that the low-redshift observations allow Bimetric gravity that behaves differently than  $\Lambda$ CDM. This motivates us to study the behaviour of CMB fluctuations in such models and see whether they are consistent with the Planck-2018 measurements. We plan to study this in the near future.

## Acknowledgements

AAS acknowledges the funding from SERB, Govt of India under the research grant MTR/2019/000599. MPR acknowledges the funding from SERB, Govt of India under the research grant no: CRG/2020/004347. SAA is funded

by UGC non-NET Fellowship scheme. The authors also acknowledge the use of High Performance Computing facility Pegasus at IUCAA, Pune, India.

- 
- [1] A. G. Riess *et al.*, “Observational evidence from supernovae for an accelerating universe and a cosmological constant,” *The Astronomical Journal*, vol. 116, pp. 1009–1038, sep 1998.
- [2] S. Perlmutter *et al.*, “Measurements of  $\Omega$  and  $\Lambda$  from 42 High-Redshift Supernovae,” *ApJ*, vol. 517, pp. 565–586, June 1999.
- [3] B. P. Schmidt, N. B. Suntzeff, M. M. Phillips, R. A. Schommer, A. Clocchiatti, R. P. Kirshner, P. Garnavich, P. Challis, B. Leibundgut, J. Spyromilio, A. G. Riess, A. V. Filippenko, M. Hamuy, R. C. Smith, C. Hogan, C. Stubbs, A. Diercks, D. Reiss, R. Gilliland, J. Tonry, J. Maza, A. Dressler, J. Walsh, and R. Ciardullo, “The High-Z Supernova Search: Measuring Cosmic Deceleration and Global Curvature of the Universe Using Type IA Supernovae,” *ApJ*, vol. 507, pp. 46–63, Nov. 1998.
- [4] L. Amendola and S. Tsujikawa, *Dark Energy: Theory and Observations*. 2010.
- [5] T. Clifton, P. G. Ferreira, A. Padilla, and C. Skordis, “Modified gravity and cosmology,” *Phys. Rep.*, vol. 513, pp. 1–189, Mar. 2012.
- [6] S. Nojiri and S. D. Odintsov, “Unified cosmic history in modified gravity: From F(R) theory to Lorentz non-invariant models,” *Physics Reports*, vol. 505, pp. 59–144, aug 2011.
- [7] L. Perivolaropoulos and F. Skara, “Challenges for  $\Lambda$ CDM: An update,” *arXiv e-prints*, p. arXiv:2105.05208, May 2021.
- [8] Planck Collaboration, P. A. R. Ade, *et al.*, “Planck 2015 results. XIII. Cosmological parameters,” *A&A*, vol. 594, p. A13, Sept. 2016.
- [9] Planck Collaboration, N. Aghanim, *et al.*, “Planck 2018 results. VI. Cosmological parameters,” *A&A*, vol. 641, p. A6, Sept. 2020.
- [10] S. Weinberg, “The Cosmological Constant Problems (Talk given at Dark Matter 2000, February, 2000),” *arXiv e-prints*, pp. astro-ph/0005265, May 2000.
- [11] A. G. Riess, L. M. Macri, S. L. Hoffmann, D. Scolnic, S. Casertano, A. V. Filippenko, B. E. Tucker, M. J. Reid, D. O. Jones, J. M. Silverman, R. Chornock, P. Challis, W. Yuan, P. J. Brown, and R. J. Foley, “A 2.4% Determination of the Local Value of the Hubble Constant,” *ApJ*, vol. 826, p. 56, July 2016.
- [12] B. Follin and L. Knox, “Insensitivity of the distance ladder Hubble constant determination to Cepheid calibration modelling choices,” *MNRAS*, vol. 477, pp. 4534–4542, July 2018.
- [13] S. Dhawan, S. W. Jha, and B. Leibundgut, “Measuring the Hubble constant with Type Ia supernovae as near-infrared standard candles,” *A&A*, vol. 609, p. A72, Jan. 2018.
- [14] M. Fierz and W. Pauli, “On Relativistic Wave Equations for Particles of Arbitrary Spin in an Electromagnetic Field,” *Proceedings of the Royal Society of London Series A*, vol. 173, pp. 211–232, Nov. 1939.
- [15] D. G. Boulware and S. Deser, “Can Gravitation Have a Finite Range?,” *Phys. Rev. D*, vol. 6, pp. 3368–3382, Dec. 1972.
- [16] C. de Rham, G. Gabadadze, and A. J. Tolley, “Resummation of Massive Gravity,” *Phys. Rev. Lett.*, vol. 106, p. 231101, June 2011.
- [17] S. F. Hassan and R. A. Rosen, “Bimetric gravity from ghost-free massive gravity,” *Journal of High Energy Physics*, vol. 2012, p. 126, Feb. 2012.
- [18] M. von Strauss, A. Schmidt-May, J. Enander, E. Mörtsell, and S. Hassan, “Cosmological solutions in bimetric gravity and their observational tests,” *Journal of Cosmology and Astroparticle Physics*, vol. 2012, pp. 042–042, mar 2012.
- [19] E. Mörtsell and S. Dhawan, “Does the Hubble constant tension call for new physics?,” *J. Cosmology Astropart. Phys.*, vol. 2018, p. 025, Sept. 2018.
- [20] S. Dhawan, A. Goobar, E. Mörtsell, R. Amanullah, and U. Feindt, “Narrowing down the possible explanations of cosmic acceleration with geometric probes,” *Journal of Cosmology and Astroparticle Physics*, vol. 2017, pp. 040–040, jul 2017.
- [21] M. Låback, A. Schmidt-May, and J. Weller, “Physical parameter space of bimetric theory and SN1a constraints,” *Journal of Cosmology and Astroparticle Physics*, vol. 2020, pp. 024–024, sep 2020.
- [22] M. Håggå and E. Mörtsell, “Constraints on bimetric gravity. part II. observational constraints,” *Journal of Cosmology and Astroparticle Physics*, vol. 2021, p. 002, may 2021.
- [23] M. Håggå and E. Mörtsell, “Constraints on bimetric gravity. part i. analytical constraints,” *Journal of Cosmology and Astroparticle Physics*, vol. 2021, p. 001, may 2021.
- [24] K. Max, M. Platscher, and J. Smirnov, “Gravitational Wave Oscillations in Bigravity,” *Phys. Rev. Lett.*, vol. 119, p. 111101, Sept. 2017.
- [25] P. Brax, A.-C. Davis, and J. Noller, “Gravitational waves in doubly coupled bigravity,” *Phys. Rev. D*, vol. 96, p. 023518, July 2017.
- [26] M. Högås and E. Mörtsell, “Constraints on bimetric gravity from Big Bang nucleosynthesis,” *arXiv e-prints*, p. arXiv:2106.09030, June 2021.
- [27] E. Di Valentino, A. Mukherjee, and A. A. Sen, “Dark Energy with Phantom Crossing and the H0 Tension,” *Entropy*, vol. 23, p. 404, Mar. 2021.
- [28] A. Chudaykin, D. Gorbunov, and N. Nedelko, “Exploring  $\Lambda$ CDM extensions with SPT-3G and Planck data:  $4\sigma$  evidence for neutrino masses, full resolution of the Hubble crisis by dark energy with phantom crossing, and all that,” *arXiv e-prints*, p. arXiv:2203.03666, Mar. 2022.
- [29] L. Amendola and C. Quercellini, “Skewness as a test of the equivalence principle,” *Physical Review Letters*, vol. 92, may 2004.
- [30] R. Emy Fazolo, L. Amendola, and H. Velten, “Skewness as a test of dark energy perturbations,” *arXiv e-prints*,

- p. arXiv:2202.08355, Feb. 2022.
- [31] M. Lüben, A. Schmidt-May, and J. Weller, “Physical parameter space of bimetric theory and SN1a constraints,” *J. Cosmology Astropart. Phys.*, vol. 2020, p. 024, Sept. 2020.
  - [32] S. Dhawan, D. Brout, D. Scolnic, A. Goobar, A. G. Riess, and V. Miranda, “Cosmological Model Insensitivity of Local  $H_0$  from the Cepheid Distance Ladder,” *ApJ*, vol. 894, p. 54, May 2020.
  - [33] A. A. Sen, S. A. Adil, and S. Sen, “Do cosmological observations allow a negative  $\Lambda$ ?” *MNRAS*, Oct. 2022.
  - [34] T. Multamaki, E. Gaztanaga, and M. Manera, “Large scale structure in nonstandard cosmologies,” *Mon. Not. Roy. Astron. Soc.*, vol. 344, p. 761, 2003.
  - [35] A. Lue, R. Scoccimarro, and G. Starkman, “Differentiating between modified gravity and dark energy,” *Phys. Rev. D*, vol. 69, p. 044005, Feb. 2004.
  - [36] Y.-S. Song and W. J. Percival, “Reconstructing the history of structure formation using redshift distortions,” *J. Cosmology Astropart. Phys.*, vol. 2009, p. 004, Oct. 2009.
  - [37] S. Nesseris, G. Pantazis, and L. Perivolaropoulos, “Tension and constraints on modified gravity parametrizations of  $G_{eff}(z)$  from growth rate and Planck data,” *Phys. Rev. D*, vol. 96, p. 023542, July 2017.
  - [38] F. Bernardeau, S. Colombi, E. Gaztañaga, and R. Scoccimarro, “Large-scale structure of the universe and cosmological perturbation theory,” *Physics Reports*, vol. 367, pp. 1–248, sep 2002.
  - [39] D. Foreman-Mackey, D. W. Hogg, D. Lang, and J. Goodman, “emcee: The MCMC hammer,” *Publications of the Astronomical Society of the Pacific*, vol. 125, pp. 306–312, mar 2013.
  - [40] D. Brout *et al.*, “The Pantheon+ Analysis: Cosmological Constraints,” *Astrophys. J.*, vol. 938, no. 2, p. 110, 2022.
  - [41] E. Macaulay, I. K. Wehus, and H. K. Eriksen, “Lower Growth Rate from Recent Redshift Space Distortion Measurements than Expected from Planck,” *Phys. Rev. Lett.*, vol. 111, no. 16, p. 161301, 2013.
  - [42] S. Alam *et al.*, “Completed SDSS-IV extended Baryon Oscillation Spectroscopic Survey: Cosmological implications from two decades of spectroscopic surveys at the Apache Point Observatory,” *Phys. Rev. D*, vol. 103, no. 8, p. 083533, 2021.
  - [43] M. J. Reid, J. A. Braatz, J. J. Condon, L. J. Greenhill, C. Henkel, and K. Y. Lo, “The Megamaser Cosmology Project: I. VLBI observations of UGC 3789,” *Astrophys. J.*, vol. 695, pp. 287–291, 2009.
  - [44] R. K. Sachs and A. M. Wolfe, “Perturbations of a Cosmological Model and Angular Variations of the Microwave Background,” *ApJ*, vol. 147, p. 73, Jan. 1967.
  - [45] A. J. Nishizawa, “The integrated Sachs-Wolfe effect and the Rees-Sciama effect,” *Progress of Theoretical and Experimental Physics*, vol. 2014, p. 06B110, June 2014.
  - [46] R. G. Crittenden and N. Turok, “Looking for a Cosmological Constant with the Rees-Sciama Effect,” *Phys. Rev. Lett.*, vol. 76, pp. 575–578, Jan. 1996.
  - [47] A. Krolewski and S. Ferraro, “The Integrated Sachs Wolfe effect: unWISE and Planck constraints on dynamical dark energy,” *J. Cosmology Astropart. Phys.*, vol. 2022, p. 033, Apr. 2022.
  - [48] M. Takada and B. Jain, “The impact of non-Gaussian errors on weak lensing surveys,” *MNRAS*, vol. 395, pp. 2065–2086, June 2009.